Monitoring of the foundations of a coastal structure submitted to breaking waves: occurrence of momentary liquefaction

David Bonjean, Pierre Foray, I. Piedra-Cueva, Hervé Michallet, P. Breul, Y. Haddani, Mathieu Mory, Stéphane Abadie

Monitoring of the foundations of a coastal structure submitted to breaking waves : Occurrence of momentary liquefaction

D. Bonjean[1], P. Foray[1], I. Piedra-Cueva[2], H. Michallet[3], P. Breul[4], Y. Haddani[4], M. Mory[2], S. Abadie[5]

[1] Laboratoire 3S (UJF-INPG-CNRS), Grenoble, France
[2] ENSGTI (Université de Pau et des Pays de l'Adour), Pau, France.
[3] LEGI (UJF-INPG-CNRS), Grenoble, France.
[4] LERMES - CUST, Aubière, France.
[5] LaSAGeC (Université de Pau et des Pays de l'Adour), Anglet, France

ABSTRACT.

A bunker dating from the 2nd world war that is presently on the beach due to beach retreat, was used as a coastal structure. Different instruments were deployed in its vicinity during three field experiments carried out in 2002 and 2003. The results of field experiments are presented herein. The time variation of pressure measured at different depth inside the soil was investigated. The aim of the field experiment was to check the possible occurrence of liquefaction during the erosion process of the foundations. Pore pressure measurements show the decay of the pressure variations transmitted inside the soil and are discussed in terms of momentary liquefaction occurrence.

KEY WORDS: Waves, sand, liquefaction, structure, bunker, coastal.

INTRODUCTION

Coastal structures, like caissons or breakwaters, settled on sand may be submitted to intense wave forces. In some cases, the structure may not keep its stability, due to the constant weakening of its foundations.
Theoretical models show that regular progressive wave may cause the momentary liquefaction of seabeds (Mei & Foda, 1981, Sakaï et al., 1992), but the phenomenon has not been observed in the field, as far as we know. A sensitivity analysis of these models show that gas content in the soil is a key parameter in determining whether liquefaction occurs (Gratiot and Mory, 2000). Considering liquefaction produced by waves as a possible phenomenon for inducing the sinking of solid objects in seabeds, a field experiment was undertaken to investigate whether liquefaction may also occur in scouring processes around a marine structure submitted to breaking waves.
An existing coastal structure was instrumented. Different measurements were carried out : soil pore pressure recordings, sand level localization, velocity and pressure measurements in the water. Several apparatus were also used that gave clues about sediment movement in the soil. Morphodynamic beach changes produced during each tide around the bunker and a beach profile along a line perpendicular to the frontal face of the bunker were recorded for each neap tide.
These results were obtained during three field trials carried out during autumn 2002, spring 2003 and autumn 2003. Very divers wave activity was encountered ranging from absolute calm, with almost no wave activity, to the storm that destroyed some of our instruments. Most results presented in this paper were obtained during the final field experiment trial, for which the most complete set of data was acquired in a systematic way. Unfortunately, the wave conditions were calm in September 2003. Some observations obtained for high wave conditions in April 2003 are also presented. The extensive set of data will not be presented here. The focus is, on the one hand, on the geotechnical features of this experiment : properties of the sand layer (grain size distribution, compaction tests, gas content), the bed level variations and, on the other hand, on the pore pressure measurements and the occurrence of liquefaction.

SITE DESCRIPTION

The field experiment was carried out at Capbreton, situated 30 km north of Biarritz. The Atlantic coast southwest of France is a 250 km long sandy coastline, subjected to a strong wave activity. The consequences of this wave activity are a mean longshore drift towards the south, which varies between 200.000 m^3/year and 630.000 m^3/year (Howa et al., 1999), and a beach retreat observed at many places along the coast. The process of beach retreat is especially significant south of the harbour pass of Capbreton. The natural longshore sediment transport was largely modified since 1974 when a jetty was build for protecting the entrance of the harbor. Bunkers, that were settled on the dune during the 2nd world war, are now located on the beach.
A bunker was chosen for conducting a field experiment to study scour and liquefaction occurrence in the vicinity of the structure. At low tide, the bunker was totally uncovered and at high tide surrounded by water with a mean water depth of about 2 m. Sets of data were acquired during each tide. The occurrence of liquefaction and scour was investigated successively during the field trial at two different local positions around the bunker. Measurements were first carried out at the middle of the bunker wall facing the sea. Figure 1 shows an inshore oriented photograph of this face of the bunker, taken during an incoming tide when the water begins surrounding the bunker. Measurement systems described later are visible on this photograph.

Figure 1. Bunker wall facing the ocean

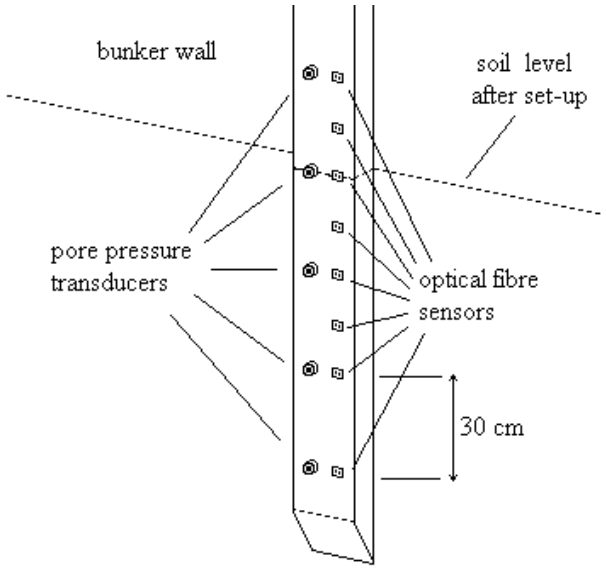

Figure 2. Diagram of the instrumented beam.

INSTRUMENTAL SETUP

Pore pressure transducers

The pressure in the water layer and inside the soil are measured from five pressure sensors implemented in a vertical beam fixed on the bunker. Druck PDCR 4030 pressure sensors are used. They allow the measurement of a relative pressure up to 7.10^4 Pa with a precision of 0.08%. This corresponds to an accuracy in the water height of about 0.5 mm.

The transducers are fixed every 30 cm along the beam (see Fig. 2). Pore pressure within the soil is transmitted to the sensitive chamber of each transducer through a porous stone. During the installation, special attention is pad to filling the volume between the porous stone and the sensitive membrane of the transducers with water. The beam itself is strongly linked to the bunker by means of several rawplugs deeply inserted in the concrete, making any relative movement between the beam and the bunker impossible.

The beam is set at neap tide by excavating a large volume of sand until the depth of the water level is reached. The beam is then pushed deeper into the soil, about 50 centimeters more, until the lowest sensor is roughly at a depth of one meter.

The excavation is finally refilled with sand which is roughly compacted by trampling it underfoot. Measurements are carried during 5 to 6 tidal periods and the degree of soil compaction is characterized from penetrometer measurements performed at each neap tide. They are compared to measurements in undisturbed soil in order to estimate the conditions when initial compaction properties are regained.

Devices for Detection of Soil Level

The pole. A graduated steel pole is used to estimate the bed level variations during high tide. The pole is initially stood on the sand bed, falls down when erosion or liquefaction occurs. The position of the pole indicates the level of the soil with bearing ability. By means of pulleys and rope, it is possible to lift up the pole from the beach during the tidal periods of recording and therefore follow the variations of the soil position.

The optic system. The sediment transport at the toe of a coastal structure submitted to breaking waves is generally very difficult to observe. Due to suspension and aeration, it is often impossible to visualize the bed level. In order to estimate the behaviour of the soil under breaking wave action, an optical system was designed in the course of the study. 5 optical fibre sensors were placed in the beam nearby the locations of pressure measurements. 3 additional sensors were located in-between the 4 upper pressure sensors (see Fig. 2). Each sensor is constituted of two optical fibres set in parallel inside the steel beam, the fibre tips facing outside the beam. One of the fibres is the light emittor, the other one receives the backscattered light. Depending on the reflected light level, it is possible to determine the presence or absence of the soil in front of the sensor. To remove surrounding light effects, the incoming light is switched alternatively on and off (frequency 500 Hz). The level of backscattered light when the emission is off is subtracted from the measurement when the emission is on.

Since the sediment colour and size vary in field conditions, any calibration to estimate the sediment concentration is unrealistic (Fig. 3). However, the optic fibre systems allows to distinguish different cases : (i) if the sensor is in the soil or not; (ii) if there is grain movement in the soil; (iii) if there are changes in the water column. Unfortunately, air bubbles and particles both reflect the light, and the discrepancy in the response between both has not been perfectly determined yet. Large fluctuations are interpreted as variations in the suspension concentration or air bubbles due to the breaking waves.

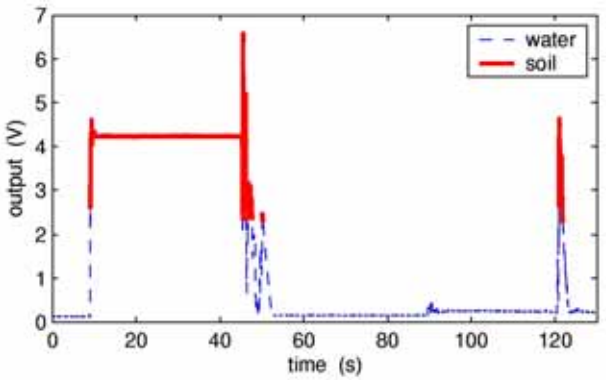

Figure 3. Typical response of an optical sensor to a calibrating test. The beam has been laid horizontally in the water, sensors facing upwards. Sand is poured on the sensors at t = 9 s. The response of the system is a rapid increase. The beam is then turned upside down to let the sand fall at t = 45 s. We note that it takes a few seconds for the output to stabilize at the minimum level corresponding to clear water. The beam is then turned to the side. At t = 120 s, a cloud of sand is dropped in front of the sensor. For this sensor, the threshold level has been set to 2.5 V.

Geoendoscopic camera.

Geoendoscopy has been developed and used for several years (Breul, 1999), in order to provide in situ soil characterization. This technique uses a video-endoscope (8,6 mm diameter). Video images are acquired from a cavity in the soil. Signal treatment or image analysis processing enable to determine different soil parameters (particle size and shape analysis, void ratio, shape of particles, orientation contact….). The video endoscope technique is usually associated with classical geotechnical tests such as penetration tests. Information obtained from image analysis can be coupled with the mechanical parameters measured at the same place.

Our primary motivation in using geoendoscopy in our field trial at Capbreton was to observe the presence of gas inside the soil during a tide and possibly evaluate the gas content at different depths. A 14 mm diameter plexiglas tube was fixed on the bunker and buried inside the soil (Figure 4b). The end of the tube inside the soil is closed. The video-endoscope can be freely displaced inside the tube to monitor the soil at different depths. Eight tests have been carried out at different locations around the bunker with depths ranging from 0 to 1,10 m below the soil surface.

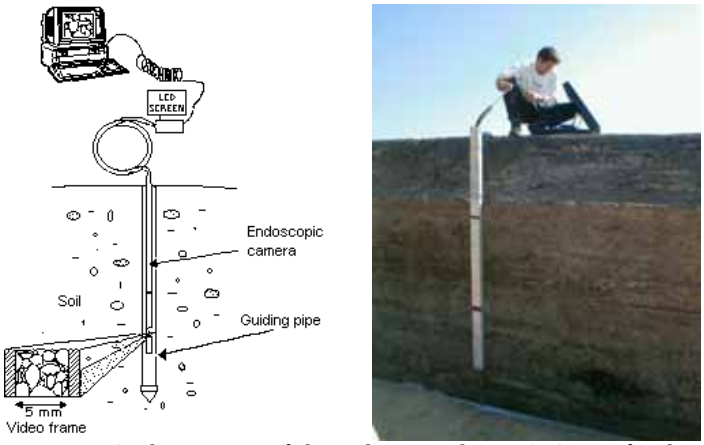

Figures 4a & 4b. Diagram of the endoscopic device & Set-up for the video-endoscope on the bunker wall.

Geoendoscopy was only available during the final field trial (autumn 2003). Significant results regarding gas content were obtained and the technique appears very promising. However, because the sea was calm during this field trial, some other observations made using geoendoscopy, such as estimations of mobile layers on top of the soil, may not be representative of what is obtained for high wave conditions. Images of 25 mm² area with a 10 folds magnification were acquired (see Fig. 5a). From the recorded images, several signal treatments which are not discussed in this paper were used in order to automatically analyse the soil and extract information about the soil parameters : size of gas bubbles and particles, contact orientations,…Figure 5b shows an example of automatic extraction of air bubbles from the picture shown in figure 5a.

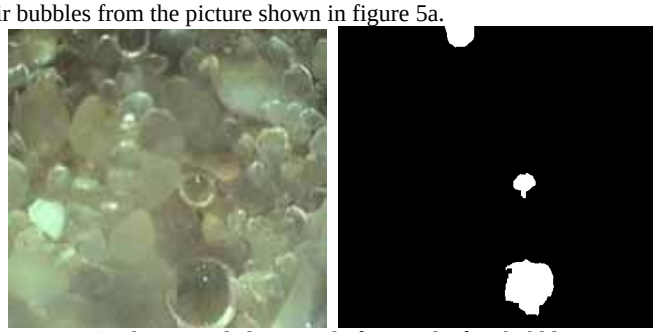

Figure 5a & 5b. Recorded image before and after bubble extraction analysis

Penetrometer.

A light dynamic penetrometer (the PANDA©) developed by the design office Sols-Solutions, was used to investigate the soil around the bunker. A steel rod is forced into the sand using a calibrated hammer with a known mass. A computer calculates the kinetic energy of the impact and the corresponding penetration, and then computes the dynamic peak resistance Q_d according to the Dutch Formula. For a given grain size distribution, the peak resistance Q_d can be directly interpreted in terms of density.

SOIL CHARACTERISTICS IN THE VICINITY OF THE BUNKER

Grain size distribution

Sand samples have been taken in the vicinity of the bunker to determine the sediment size distribution. The appearance of the sand on the beach is homogeneous so that the distribution is representative of the sand properties in the area investigated. The mean sediment size is $d_{50} = 0.35$ *mm*. Most of the sand is contained in a narrow size band as indicated by the value of the uniformity coefficient $C_u = d_{60} / d_{10} = 1.77$, *where* $d_{10} = 0.22$ *mm* and $d_{60} = 0.39$ *mm.*
The sand distribution did not appear to vary significantly with time. The intermittent deposition of limited quantities of gravel of a few mm in diameter on the sandy bed was only noticed on some occasions.

Penetrometer Tests around the Bunker

Penetrometer tests were carried out very close to the position of investigations in order to evaluate the density profiles of the soil and their evolution after the tides. The disturbance produced by the installation of the beam makes the soil looser as compared to an indisturbed initial soil whose properties are presumably regained after several tidal periods. Several bunkers are left on the beach. The results presented in this paper were obtained around the so-called “central bunker”, but at each neap tide additional penetrometer tests were carried out at the middle of the wall facing the ocean of the so-called “southern bunker”. The buildings of the central and southern bunkers are similar. They are settled on the beach with the same orientation, and at the same distance from the shoreline. Thus it can be reasonably assumed that a comparison between penetrometer tests realized on both bunkers makes sense. The southern bunker was never instrumented. The soil investigated in its vicinity was never disturbed by our experiments. All the tests performed there give a good reference of the dynamic resistance of a natural beach just in front of a coastal structure. By comparing the penetrometer profiles in undisturbed soil and at the instrument locations it has been possible to quantify the time required by the soil to recover its initial properties. Additional penetrometer tests were achieved in the vicinity of the central bunker in order to estimate the spatial variability of the geotechnical properties of the soil induced by the bunker.

Penetrometer profiles in undisturbed soil.

A typical example of a dynamic resistance profile versus depth measured in front of the southern bunker is shown in figure 6. During the first tens of centimeters of penetration, the dynamic resistance is increase gradually. The average value of the resistance around one meter depth is always in the range 2 MPa - 5 Mpa for a non-disturbed soil. Below a depth of 2 m, the resistance may reach a value of 5 MPa, or even more depending on the date of the test. The plot shown in figure 6 is very irregular at this depth and indicates the presence of a significant amount of gravel. The increase in the penetration resistance can be due to a higher density or a change in grain size (larger grains generally induce higher resistance values).

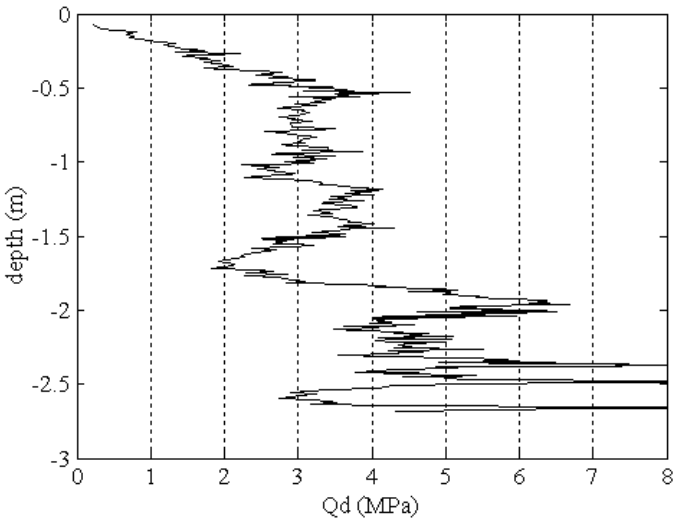

Figure 6. Penetrometer profile in undisturbed soil.

Laboratory penetration tests performed with the Dynamic PANDA System have shown that for sands the dynamic resistance Qd is very close to the classical tip resistance Qc measured by a standard static Cone Penetration Test (CPT). Thus, the correlations established for the CPT can be used to evaluate the density profiles of the soil. Nevertheless, as mentioned by Puech and Foray (2002) the low level of depth has to be taken into account in the correlations, and an equivalent "steady-state" value of the tip resistance has to be estimated. The following expression, determined from CPT tests performed at shallow depth in the large 3S Calibration Chamber was used to evaluate the average density index (I_D) of the first meter layer from the corresponding steady-state value of the tip resistance Q_c.

$$I_D = 0.209 \ln Q_c + 0.25 \quad (Q_c \text{ in MPa}) \qquad (1)$$

Using this procedure, at depths between 1 and 2m in the middle part of the wall facing the ocean, values of Qd between 2 and 5 Mpa should correspond to density indexes in the range of 35 to 55%.

Foray et al (2002) compared values of small strain shear modulus of the sand obtained from crosshole geophysical tests with the values of the cone tip resistance at the same shallow depth in the Calibration Chamber. From this correlation, the small strain shear modulus G_{max} of the soil field profile with Q_d between 3 to 5 MPa was estimated to be in the order of 20 MPa.

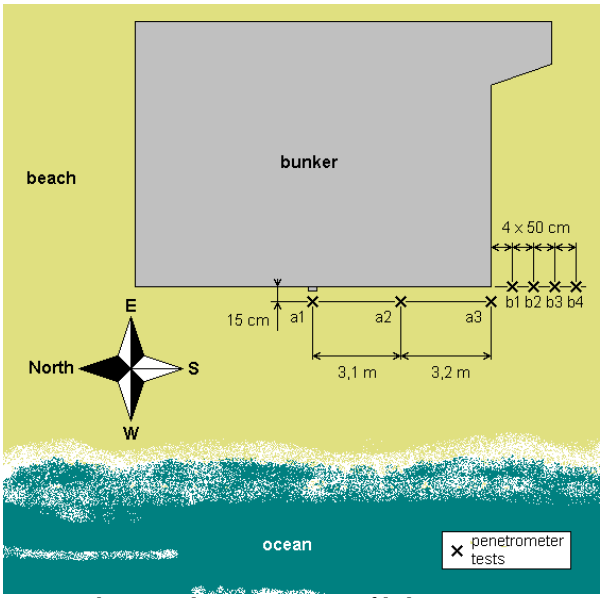

Figure 7. Beach map and penetrometer profile locations.

Spatial variability of penetration properties around the bunker. Due to the short lapse of time left at neap tide, it is not possible to investigate with the PANDA the whole subsoil around the bunker . One or two vertical profiles could usually be measured during this period. However, penetration profiles were measured at different locations along several lines parallel or perpendicular to the lateral bunker walls, as shown in figure 7. The profiles presented in figures 8 and 9 were obtained in April 2003. Very strong wave conditions were achieved during this field trial and significant bed level variations were observed during each tidal periods. This strong wave activity directly implies the formation of a very loose layer from 0,50 m thick in the middle of the wall facing the ocean to 1,5 m in the corner, with a density index around 25%. Moreover, the loose sandy layer gets thinner as the measurement is made further from the bunker (see Fig. 9).We attribute its existence to a scouring effect, related to waves intensity, that digs a gap all around the bunker at high tide, which is filled again with sediment as the sea retreats. In comparison the profile presented in figure 6 was performed after a period of very weak wave activity, and where that loose layer is not visible. A similar process is seen in Figure 12 by the accretion noticed at the end of the recording plotted, although its magnitude is smaller due to the calm wave conditions of the September 2003 field trial.

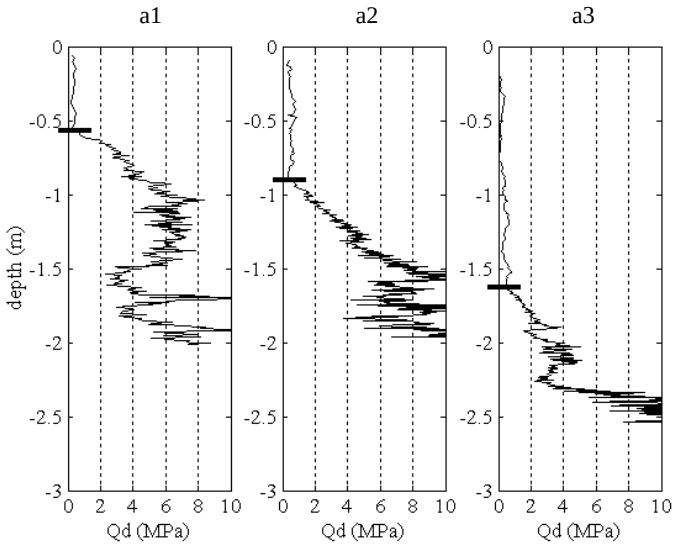

Figure 8. Vertical penetration profiles along the wall facing the ocean.

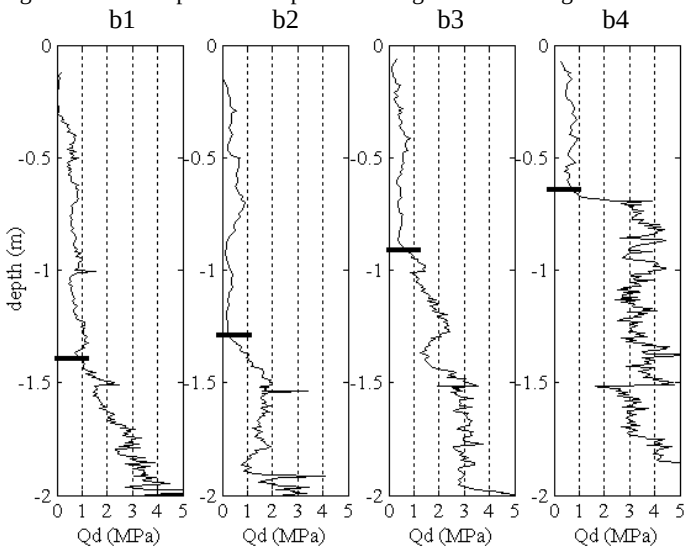

Figure 9. Vertical penetration profiles in the corner.

Evolution with time of the soil density after setting-up the Pore Pressure Transducers. Figure 10 presents three vertical penetrometer profiles measured at the same location for three successive neap tides after the installation of the beam. Although the sand used to re-fill the installation hole was slightly compacted, a thin layer of very loose sand remained between the depths 1.0 m and 1.2 m. This was the position of the water level at neap time and, therefore, it was impossible to compact the sand efficiently. This looser layer is still visible after one tide. After two tides this layer disappeared and the average penetration resistance at one meter depth reached values in the range 2 MPa - 5 MPa., typical of those found for the undisturbed seabed, as shown before. Thus, it can be assumed that the duration of two tides (e.g. 12 hours) is sufficient to regain a compaction state of the soil in the vicinity of our instruments similar to that observed in undisturbed soil.

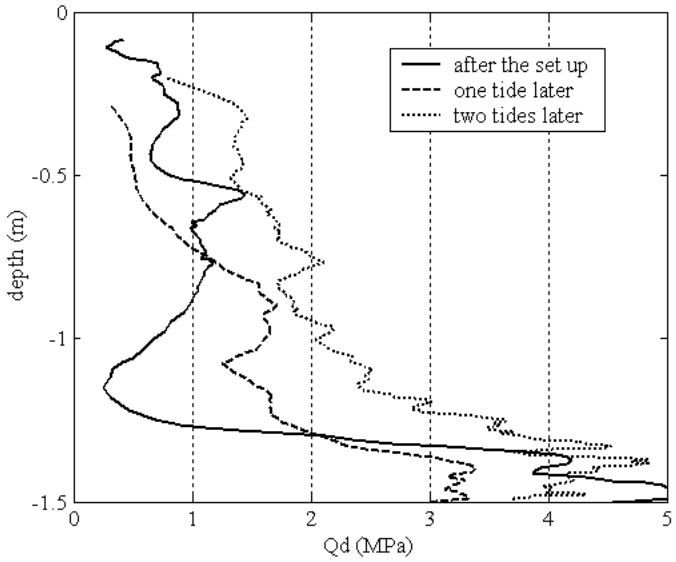

Figure 10. Evolution with time of pit resistance profiles.

Air content.

The major result of the geoendoscopic tests is the evidence given of a significant presence of gas deep inside the soil (see Fig. 5a & 10) ,down to 50 cm in the case investigated. Gas content is not constant with depth. A thin layer of about 10 cm saturated with water is observed on top of the soil. Gas is confined below down to about 60 cm, and remains in this state during all the tide, although some escape of gas bubbles to the surface was observed during the tide. Below this layer of unsaturated soil, which roughly corresponds to the layer of sand drained at neap tide, saturated soil is again observed. The thickness of the saturated layer on top of the soil is obviously linked to the mobility of sand produced by waves which enhance the upward escape of bubbles.

Figure 11 shows the variation of gas content with depth. The “surface gas content ratio” is plotted, computed as the ratio of the area filled in with gas bubbles to the total image area.

The “Surface gas content” is a non physical value, and it is very difficult to calculate a volumetric gas content ratio from it. An accurate calibration is still needed to determine correlations between this surface gas content ratio and the volumetric one, first. That would then enable to calculate a saturation degree.

SOIL DETECTION DURING HIGH TIDE

Comparisons between the optical and the graduated pole measurements are shown in figure 12 for a duration covering a tidal period. The minimum and maximum values of the optical sensor output voltage is

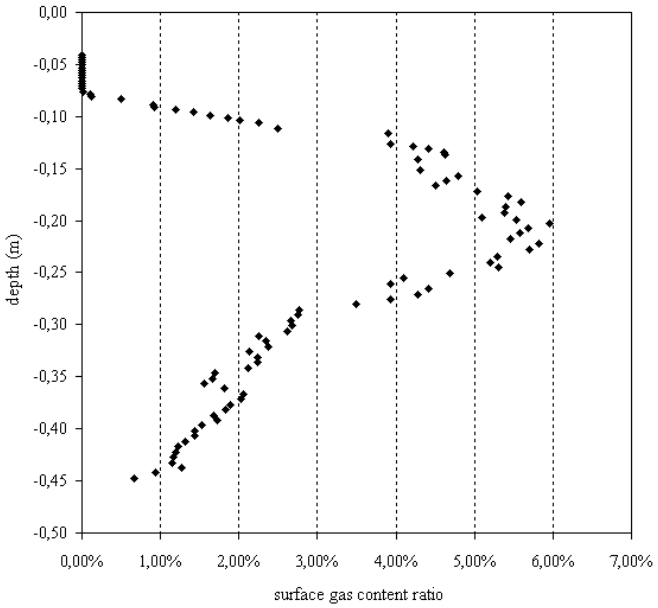

Figure 11. Surface gas content ratio versus depth.

computed over 10 min sequences. If the minimum is above the threshold value, the sensor is considered in the soil (shown as squares and stars in Fig. 12). If the difference between maximum and minimum is large, movements (in the soil or in the water) are deduced. The bed level estimates from the optical system and graduated pole are in good agreement. The mean and maximum water levels deduced from the pressure sensors are also shown. Clearly, at the beginning of the tide, waves are breaking against the bunker and erosion occurs. At high tide (between 16:00 and 18:00), the waves break over the bunker and the soil does not change much. When the water level is lower (18:30 – 19:00), the waves are breaking again against the bunker: erosion is measured. At the end of the tide (after 19:00), accretion is observed.

The soil level detection system allows to determine which pore pressure transducers are in the soil, and which ones are in the water layer. This is a key issue for interpreting pore pressure measurements.

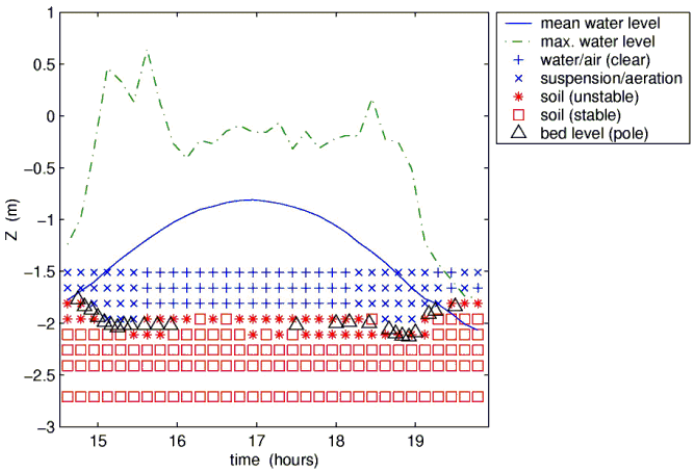

Figure 12. Evolution of the soil versus water level and wave activity during a tide, averaged over periods of 10 min. Z = 0 is the top of the bunker. 8 optical sensors were located each 15 cm from Z = -151 cm to Z = -241 cm and at Z = -271 cm. The soil position at the preceding low tide was at z = -178 cm.

The stable soil level during the tide evolve between z = -150 cm and z = -220 cm, that confirms the CPT results showing a disturbed area between 50 cm and 150 cm deep.

PORE PRESSURE RECORDINGS ANALYSIS

For the measurements presented in this part (see Fig 12a), three pressure sensors were located inside the sandy bed at positions that were -90 cm, -60 cm and -30 cm below the bed level during the main part of the tide duration. The fourth and the fifth ones were placed approximately at the position of the bed level and at a distance of 30 cm above the bed, respectively.

Figure 13a presents a time series of pore pressure measurements. The absolute pressure is plotted in Figure 13a and therefore, the pressure variations having the maximum and minimum averaged values were measured by the lowest and highest pressure sensors implemented in the vertical beam, respectively. This time series covers a duration of about two wave periods during which the three lowest sensors p_5, p_4 and p_3 were inside the soil. The upper sensor p_1 remained in the water layer and the position of sensor p_2 corresponds approximately to the bed surface. The plots in Figure 14a display a clear damping of the pressure variations with increasing distance inside the soil. A phase shift is also noticeable; at each depth the maximum pressure is reached with a delay that increases with the distance from the bed surface level.

A spectral frequency analysis of pore pressure enables quantification of spectrum the damping of pore pressure variations inside the soil. The power spectrum of pore pressure variations is shown in Figure 13b. It was computed for the time series of the experiment shown partly in Figure 13a. Three simply related frequencies appear in the frequency spectrum. The decay of pressure variations with increasing distance inside the soil is easily determined by comparing the value of the power spectrum measured at different levels for each frequency. The power spectra measured by the pressure sensors p_1 and p_2 are almost identical. This is an expected result because the two sensors are in the water layer and they are only separated by a distance of 30 cm. The decay inside the soil is shown in Figure 14a as the ratio versus frequency of the power spectrum level measured for the pressure sensors located inside the soil (p_3, p_4 and p_5) to the power spectrum level measured by the pressure sensor p_2 located near the bed surface.

A set of equations that compute the wave-induced effective stress in seabed was published by Sakai, Hatanaka and Mase (1992). This model actually originates from a former work by Mei and Foda (1981). It describes the variation in time of pore pressure in the seabed when a monochromatic wave passes over an elastic plane sandy bed. This geometry is different from ours, but we found it of interest to compare the decay of pore pressure variations measured in the field to the decay predicted by Sakaï *et al.* equations. The pore pressure variation inside the bed is given by eq. (2) of Sakaï et al.

$$\frac{P(z)}{Po}=\left[\frac{1}{1+m}e^{-\lambda z}+\frac{m}{1+m}e^{\frac{(i-1)z}{\sqrt{2}\,\delta}}\right]e^{i(\lambda x-\sigma t)} \qquad (2)$$

λ and σ are the wave number and frequency of the wave propagating in the water layer, respectively. The z axis is oriented downward and $z=0$ is at the bed surface. The parameters appearing in (2) are defined as follows:

$$m=\frac{n}{1-2\upsilon}\frac{G}{\beta}, \qquad \beta=\frac{1}{\beta_w}+\frac{C_{gas}}{P_{ref}} \qquad (3a)\ (3b)$$

$$\text{and}\ \delta=\left(\frac{k}{\rho g}\frac{G}{\sigma}\right)^{1/2}\left[\frac{nG}{\beta}+\frac{1-2\upsilon}{2(1-\upsilon)}\right]^{-1/2} \qquad (3c)$$

An important issue of Sakaï et al. model is the very significant sensitivity of the results to the gas content in the soil C_{gas}, as shown by Gratiot and Mory (2000). By adjusting the gas content in the soil, a set of parameters was found that provides a good comparison between the decay ratio found in the field (see Fig. 14a) and the decay ratio predicted by the Sakaï et al. equations (see Fig. 14b).

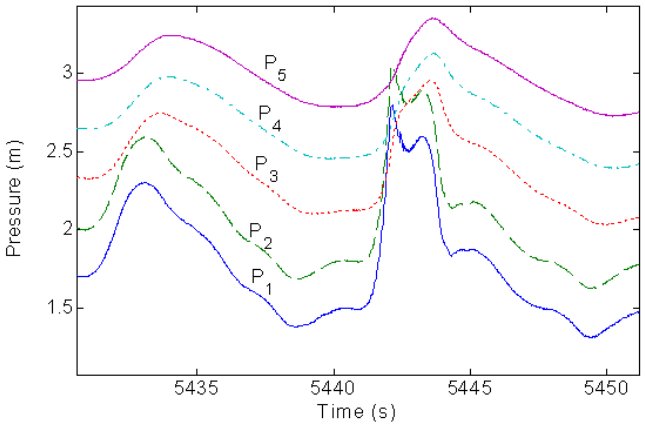

13a

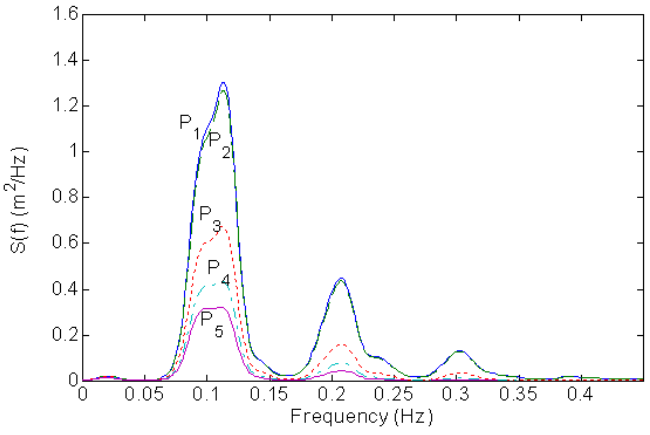

13b

Figures 13a & 13b: Time series of pore pressure variations and pressure power spectra at five different levels inside the soil and in the water layer.

This result was obtained for a bed porosity $n=0.50$ and a bed permeability $k = 2.0\ 10^{-4}\ ms^{-1}$. The elasticity of the soil was given by the shear modulus of the solid skeleton $G = 20\ MPa$ and Poisson modulus $\nu = 0.498$. β is the coefficient of compressibility of water and P_{ref} is the averaged level of pressure. The plot shown in Figure 14b was obtained for $C_{gas} = 0.01$.

Although the cases investigated in the field and the configuration studied by Sakaï *et al*. are different, the comparison between Figure 14a and 14b is reasonably good. The decrease of the decay coefficient with increasing frequency is similar in the two figures and the orders of magnitude of decay measured in the field are predicted by a simple application of Sakaï *et al*. model. The level of gas content $Cgas = 0.01$ required to predict the significant damping of pressure inside the soil measured in the field is high. This predicts the presence of significant gas inside the soil. This conclusion is in agreement with the visual observations of gas content.

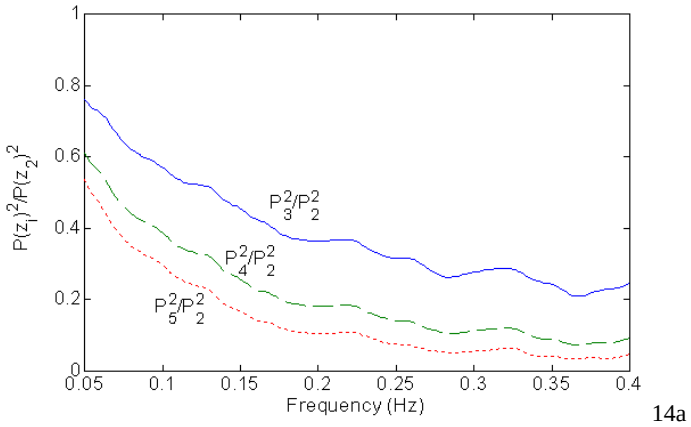

14a

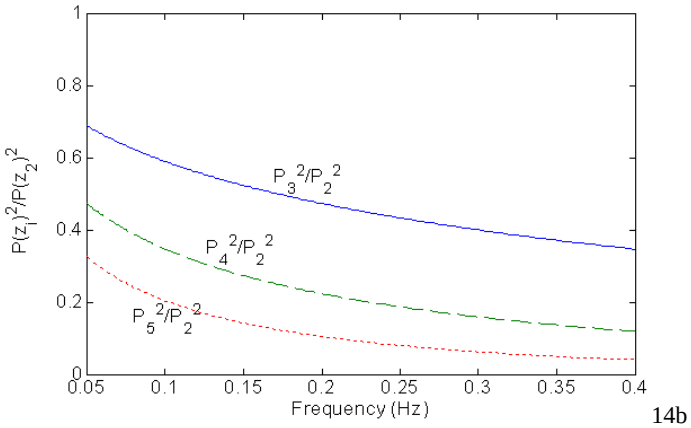

14b

Figures 14a & 14b: Variations with frequency of the damping coefficient of pressure variations at three different levels inside the soil, experimental & predicted by Sakai's equations.

LIQUEFACTION EVENTS

Uplift hydraulic gradients

The attenuation and decay in the transmission of pore pressure in soil induces a non hydrostatic pressure distribution in the seabed, causing either an upward or downward hydraulic gradient when the hydrostatic equilibrium state is disturbed.

Figure 15a presents a pore pressure recording from May, 6th 2003 at 5:00 AM. The first pore pressure transducer (pp1) was above the sand, and the four others were in the seabed. Figure 15b plots the difference between two consecutive transducers. The distance between both is equal to 30 cm. In a fluid at an hydrostatic equilibrium state, this difference should remain constant and equal to –3 kPa. We observed that each wave disturbs that equilibrium and generate an upward gradient which is favourable to instability of sand grains, and may help scour. It is sometime strong enough to counter the effective weight of the layer of sand concerned, and then liquefy it. One of those events is plotted on Figures 15a&b. (The critical upward gradient was calculated with an effective weight of the sand γ' equal to 9 $kN.m^{-3}$.) This kind of event occurred for each survey period. The highest wave conditions induced liquefaction to occur more often, and the liquefied layer to be thicker.

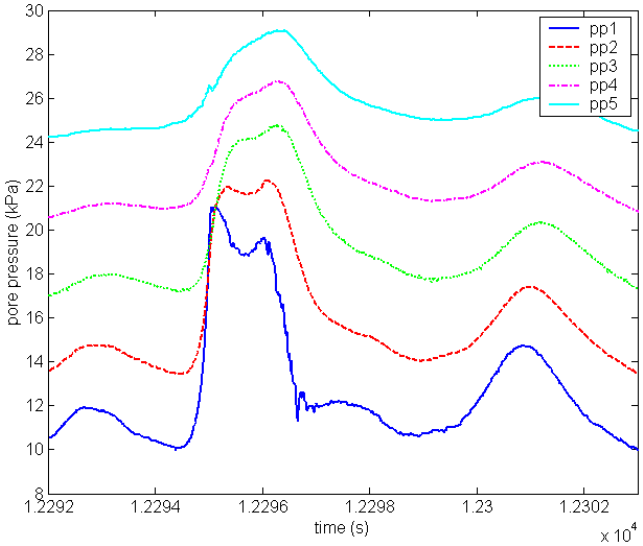

15a

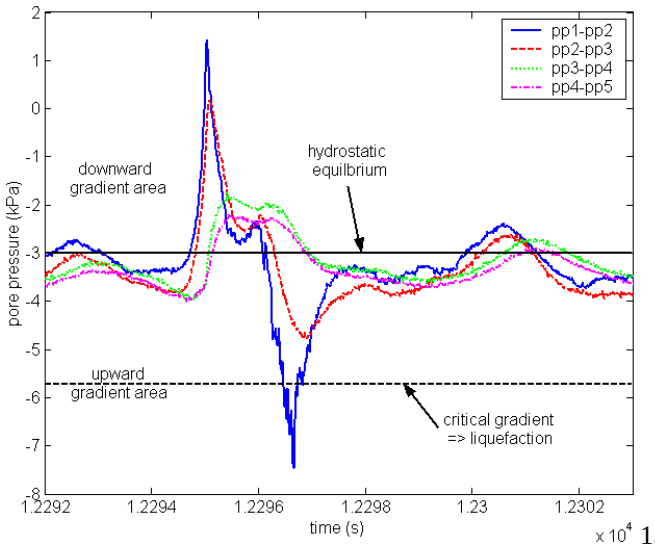

15b

Figure 15a &15b. Pore pressure transducers response at the time scale of a wave. An example of a liquefaction event.

Endoscopic observations

During high tide period, endoscopic investigations gave very interesting information about the sandbed to the wall facing the ocean. Those investigations were performed quite near to the pore pressure transducers and the other measurement devices, and close to the middle of the wall facing the ocean. Thus we can assume that the observations recorded are similar to the ones that occurred in front of the other instruments.

It is possible to observe the limit between the sandbed and the water, when no wave is breaking and the water is carrying low suspension.

But it is also possible to observe the displacements of the sand grains, within a mobile layer, and the thickness of this mobile layer. Then we can determine, for any wave, the part of the sandbed that is submitted to visible strains, the part of the sand that is not disturbed by the wave action, and the depth of the frontier between these two areas.

Unfortunately, during the experiment involving the geoendoscopic camera, the beach was submitted to a very weak wave activity. This phenomenon has not been be observed with high waves.

Drops of pore pressure

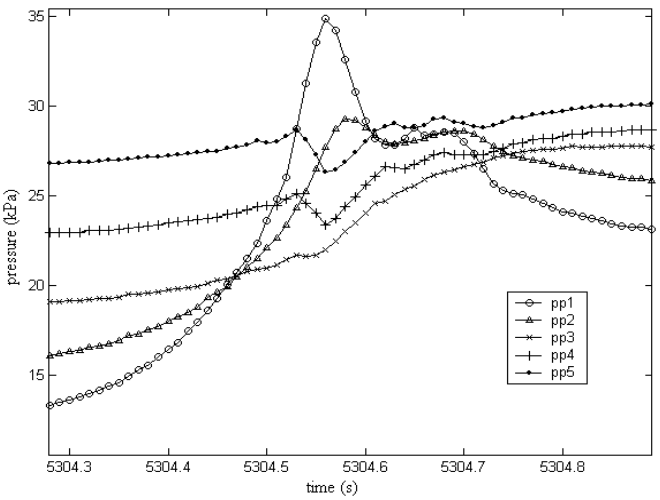

Figure 16. Drops of pressure inside the soil while a wave is breaking.

Sometimes, particular events have been recorded by the pore pressure acquisition system. For the plot in Figure 16 the pore pressure sensor pp1 is the only one above the soil level. It is interesting to notice that, while pressure in the water (pp1) increases, pp3, pp4 and pp5 display a slight drop in the pore pressure level.

Such recordings were obtained with a very strong wave activity. They occurred quite rarely, almost only for waves breaking exactly on the wall. This corresponds to the sharpest peaks of pressure in the fluid layer seen on pore pressure recordings. During this event, at the precise moment when the drop occurs, the difference between the two upper transducers (pp1 and pp2) does not indicate an uplift gradient. Such a drop of pressure suggests a volume change inside the soil. A dense sand submitted to shear strains would dilate, and then increase its void ratio, that could explain the drop recorded. Because the drop magnitude increases with increasing depth, we believe that such drops of pressure indicate major in-depth soil dilations.

CONCLUSIONS

Complete monitoring gives the sand bed level during the recording at high tide and then allows us to make an accurate comparison between pore pressure recording and analysis.

Moreover, the light penetrometer allows an in-situ survey of the bunker foundations. CPT data clearly indicates the depth of soil disturbed by the waves and highlights the influence of the location in the vicinity of the bunker, and also gives approximation of mechanical parameters of the soil around a coastal structure.

An important issue of this study is the observation of a significant amount of air bubbles trapped between the grains at low tide. This leads to conclude that the air content ratio is much higher than for deep sub-sea sandbeds that are always submerged.

Our field experiments shed light on the damping of pore pressures within the soil. Although the configurations are different, our experimental results obtained in the field are qualitatively and quantitatively similar to the analytical predictions of Sakai et al. for the damping of pore pressure inside the soil under a progressive wave.

The main point of this paper is that the mechanism of seabed liquefaction under progressive waves as described by Sakai also occurs in the vicinity of coastal structures. The delay in pore pressure transmission to the soil generates an upward hydraulic gradient which is sufficient to liquefy the sand at the foot of the bunker. Such liquefaction events were observed several times for almost every tidal period surveyed.

Considerable scour was also observed. The same mechanism of upward hydraulic gradient probably influences scour before causing liquefaction. This makes it difficult to distinguish between the actions of liquefaction and scour. However it is proven that liquefaction occurs and thus plays a role in coastal structure destabilization.

ACKNOWLEDGEMENTS

This study was partially funded by the European Commission Research Directorate, FP5, specific program “Energy, Environment and Sustainable Development”, Contract No EVK3-CT-2000-00038, Liquefaction Around Marine Structures LIMAS.
(http://vb.mek.dtu.dk/research/limas/limas.html).

REFERENCES

Breul, P (1999). *"Caractérisation endoscopique des milieux granulaires couplée à l’essai de pénétration”*, Thèse de docteur-ingénieur de l’Université de Clermont-Ferrand, pp280, Oct.1999.

Breul, P, and Gourves, R (2003). Rapports d’essais, *"Liquéfaction des sables en littoral ”*, Synthèse des essais réalisés au laboratoire 3S de Grenoble le 28 Janvier 2003 - Rapport d’essai n°1 et 2 – *LERMES* -

Foray, P, Emerson, M, and Puech, A (2002) *"Correlations between compressive seismic velocity and cone resistance at shallow penetration in sands”* Int. Conf. “Offshore Site Investigation and Geotechnics, Sustainability Through Diversity”, 26-28 nov. 2002, London

Gratiot, N, and Mory, M (2000). *"Wave induced sea bed liquefaction with application to mine burial”*, Proc. 10th ISOPE Conference, Seattle, may 28-june 2.

Howa, H, Salomon, JN, and Tastet, JP (1999). *“Littoral Aquitain”*, Acquis Sciences n°20.

Mei, CC, and Foda, MA (1981). *“Wave induced responses in a fluid-filled poroelastic solid with a free surface – a boudary layer theory”*. Geophys. J. R. Astr. Soc., Vol 66, pp.597-631.

Puech, A, and Foray, P (2002.) *“A Refined Model for Interpreting Shallow Penetration CPT’s in Sand”* Proc. Offshore Technology Conference, OTC 2002, Houston, USA, Paper OTC 14275, 12 pages.

Sakai, T, Hatanaka, K, and Mase, H (1992), *“Wave induced stresses in seabed and is momentary liquefaction”*, Proc. ASCE, J. Waterways, Port, Coastal and Ocean Engineering, 118(WW2), 202-206.